



Published in final edited form as:

Analyst. 2008 November ; 133(11): 1550–1555. doi:10.1039/b719810h.

Dye-Doped Silica Nanoparticle Labels/Protein Microarray for Detection of Protein Biomarkers

Hong Wu, Qisheng Huo, Susan Varnum, Jun Wang, Guodong Liu, Zimin Nie, Jun Liu, and Yuehe Lin

Pacific Northwest National Laboratory, Richland, Washington 99352

Abstract

We report a dye-encapsulated silica nanoparticle as a label, with the advantages of high fluorescence intensity, photostability, and biocompatibility, in conjunction with microarray technology for sensitive immunoassay of a biomarker, Interleukin-6 (IL-6), on a microarray format. The tris (2,2'-bipyridyl)ruthenium (II)chloride hexahydrate (RUBY) dye was incorporated into silica nanoparticles using a simple one-step microemulsion synthesis. In this synthesis process, Igepal CA520 was used as the surfactant, therefore, no requirement of cosolvent during the synthesis and the particle size was reduced comparing to the commonly used Triton surfactant system. The nanoparticles are uniform in size with a diameter of 50 nm. The microarray fluorescent immunoassay approach based on dye-doped silica nanoparticle labels has high sensitivity for practical applications with a limit of detection for IL-6 down to 0.1 ng mL⁻¹. The calibration curve is linear over the range from 0.1 ng mL⁻¹ to 10 ng mL⁻¹. Furthermore, results illustrated that the assay is highly specific for IL-6 in the presence of range of cytokines or proteins. The RuDS dye-labeled nanoparticles in connection with protein microarrays show the promise for clinical diagnosis of biomarkers.

Keywords

biomarker; IL-6; protein microarray; dye doped silica nanoparticles; fluorescence

1. Introduction

Biomarkers serve as indicators of biological and pathological processes, or physiological and pharmacological responses to a drug treatment.¹ In the past few years, many efforts have been focused on the discovery, identification and characterization of disease related biomarkers. Interleukin-6 (IL-6) is a pro-inflammatory cytokine that has an active role in inflammation², immunology³, bone metabolism⁴, reproduction⁵, arthritis⁶, neoplasia⁷, and aging⁸. Elevated levels of IL-6 are associated with clinical as well as subclinical cardiovascular disease⁹. The normal level in serum is in the range of 10–75 pg/ml, whereas individuals with various disease states have elevations in IL-6 levels in the ng/ml range¹⁰. High levels of IL-6 also have been correlated with prostate cancer of hormone-independent prostate cancer patients¹¹, breast cancer of AIDS patients¹², and stress¹³.

Due to the importance of biological and pathological functions of IL-6, a number of assays including, the enzyme-linked immunosorbent assay (ELISA), enzyme-linked immunospot (ELISpot) assay¹⁴, radioimmunoassay (RIA)¹⁵ and electrochemical immunoassay¹⁶, have been employed in the bioanalysis of cytokine IL-6. Recently, protein microarray technology

has attracted wide attention because of the potential to use very small sample volumes and the ability to analyze large number of samples (high throughput)¹⁷. Urbanowska group¹⁸ and Johnson group¹⁹ applied the protein microarray technology with dyes Cy3 and Cy5 as labels in monitoring of IL-6 and other cytokines, which significantly improves the sample throughput due to the high density samples in the array format. However, these methods require biotin amplification using biotinyl tyramide to attract more dye molecules, which introduces more steps and complexity into the procedure²⁰.

Recent development in nanotechnologies provides more opportunities for researchers in bioanalysis and clinical diagnosis.²¹⁻³⁰ Various synthesis approach for preparing nanoparticles and their application in bioimaging, labeling, and sensing have been reported. Silica NPs shows many advantages, e. g. ease of fabrication and functionalization, high stability in a variety of environments, and biocompatibility for the development of labels, carriers, and vehicles. Silica nanoparticles for loading probes also have a number of advantages over organic ones (e.g. polystyrene beads): (i) There are no swelling or porosity changes with changing in pH. (ii) They are nontoxic and highly biocompatible with biological systems. (iii) Their surfaces can be easily modified with different functional groups. Different strategies (e.g., covalent binding, entrapment, and electrostatic interaction) have been used to prepare functionalized silica NPs for bioimaging, diagnosis, and therapeutic applications. Organic dyes, protein, DNA, and drugs have been used to functionalize the silica NPs for specific applications. For example, fluorescent dyes and enzymes have been attached to silica NPs for cell imaging or for analyzing small biomolecules³¹; drug- and DNA-functionalized silica NPs have been evaluated as vehicles for drug and gene delivery³². Recently, Tan's group^{21, 22} used a microemulsion technique with polyoxethylene (10) isoctylphenyl nonionic surfactant (Triton X-100) for synthesizing a dye-doped silica nanoparticles which can encapsulate several thousands of dye molecules per nanoparticle. And these silica nanoparticles can be used for sensitive detection of protein biomarkers. The advances of this type of nanoparticles include the high intensity of the fluorescence, excellent photostability and good biocompatibility.

In the commonly used Triton surfactant system for microemulsion synthesis, the surfactant tends to form aggregated liquid crystalline structures and a cosolvent such as alcohol has to be used to stabilize the microemulsion due to the low solubility of the surfactant (to break the liquid crystalline structure)³³. The solubility of the hydrophilic component (water) is also very limited³⁴. In such synthesis, the silica particle sizes are very sensitive to the kind of cosolvent and cosolvent concentration, and the particle sizes are typical over 70 nm³⁵. The added alcohol also has a large effect on the hydrolysis of condensation of the silicate species³⁶.

The purpose of this paper is to develop an alternative microemulsion route for dye-doped silica nanoparticle synthesis, and to demonstrate the application of these dye-doped nanoparticles as fluorescent labels for direct detection of protein biomarkers (IL-6 was used as a model biomarker) in a protein microarray. We chose a different non-ionic surfactant system, Igepal CA520 ((C₈H₁₇)-C₆H₄-O-(CH₂-CH₂-O)₅H) and n-heptane. The CA520 and heptane system has good solubility for both the surfactant and water, and has a large, stable single phase microemulsion region in the phase diagram. The microemulsion can be directly prepared without the addition of a cosolvent (alcohol) to stabilize the microemulsion phase,²² and therefore is a more straightforward and controllable method. As an added benefit, since no alcohol is added, a fast hydrolysis rate is observed (a high alcohol to TEOS ratio usually slows down hydrolysis)³⁶, which leads to high nucleation rate and smaller particles (down to 50 nm). In the microarray approach, the captured anti-IL-6 antibodies were printed on an amino-functionalized slide with a microarrayer. The dye-doped silica NPs modified with secondary anti-IL-6 antibodies were used as labels. IL-6 in samples was detected through a sandwich immunoassay and fluorescence microarray scanner. The sensitivity and specificity of the method was examined in the presence of other proteins. Protein microarray analysis with the

antibody conjugated silica nanoparticles containing high intensity of dyes showed good sensitivity and high specificity. It provides new opportunity for clinical detection of IL-6 related diseases.

2. Experimental

2.1. Apparatus

A ScanArray Express HT microarray scanner from Packard BioScience BioChip Technologies (Billerica, MA) was used for fluorescence image and quantitative detection. Images thus captured in the ScanArray software were quantitated using ImaGene software (Biodiscovery). Fluorescence spectra were taken from a SPEX, 1680 double spectrometer. A robotic printer MicroGrid from Apogent Discoveries (Wilmslow, Cheshire, UK) was used to prepare antibody microarray. Transmission electron microscopy (TEM) image was carried out on a Jeol JEM 2010 microscope at 200 Kev. All images were digitally recorded with a slow-scan charged coupled devices camera (image size 1024×1024 pixels). Centrifugation was performed with a Sorvall RC 26 plus (Kendro Laboratory Product).

2.2. Reagents

Mouse IgG, heptane, tetraethyl orthosilicate (TEOS), acetone, ethanol, bovin serum albumin (BSA), phosphate buffer saline (0.1 M, pH 7.4) (PBS), acetic acid, 3-aminopropyltriethoxysilane (APTS), glutaric anhydride, MES hydrate, N-hydroxy succinimide (NHS), N,N-dimethylformamide (DMF), N-(3-dimethylaminopropyl)-N'-ethyl-carbodiimide hydrochloride (EDC), Igepal CA-520 and Tween-20 were purchased from Aldrich-Sigma (St. Louis, CA). 1 × PBS/casein blocking solution was purchased from Bio-RAD Laboratories (Hercules, CA). The 1 × PBS/casein blocking solution contains 1% casein. The 0.1 × PBS/casein blocking solution indicates a 10× dilution from the 1 × sample. Tris (2,2'-bipyridyl) ruthenium (II) chloride hexahydrate (Rubpy) was purchased from Strem Chemicals (Newburyport, CA). Ammonia hydroxide was purchased from Fisher Scientific (Tustin, CA). Biotin anti-mouse IL-6, purified anti-mouse IL-6, recombinant mouse IL-6, recombinant mouse IL-1 α and recombinant mouse IL-1 β were purchased from BioLegend (San Diego, CA). Recombinant mouse tumor necrosis factor alpha (TNF- α), was purchased from eBioscience (San Diego, CA). MMP-2 was purchased from EMD Biosciences, Inc. (San Diego, CA). Bis-(sulfosuccinimidyl) suberate (BS³) was purchased from Pierce Biotechnology Inc. (Rockford, IL). All of the chemicals were used as received and all stock solutions were prepared using Milipore-purified deionized or autoclaved water.

2.3. Preparation of Rubpy Doped Silica (RuDS) Nanoparticles

The nanoparticles were prepared using the microemulsion method. In a typical microemulsion for preparation of silica nanoparticles, 40 g of surfactant Igepal CA-520 was dissolved in 160 g of heptane with stirring. 35 mg of Rubpy dye was dissolved in 3.76 g of ammonium hydroxide (28–30% by weight) and 0.5 g of water, and added to the surfactant solution. Then, 0.8 g of TEOS was added with stirring. The mixture was stored in dark for 48 hours. Acetone was added to break the microemulsion and the particles were recovered by centrifugation at 10,000 RPM for 10 min. The particles were washed a few times with ethanol and finally washed with water. The size and morphology of dye-doped silica nanoparticles synthesized in W/O microemulsion were measured using a TEM. The sample for TEM was prepared by placing a few drops of the nanoparticle-containing solution on carbon-coated copper grids. After evaporation of the solvent, the particles were directly observed at an operating voltage of 200 keV.

2.4. Preparation of Anti-IL-6 Conjugated RuDS Nanoparticles

In order to conjugate with biomolecules, RuDS nanoparticles were functionalized with carboxyl groups. Two milligrams of fluorescent silica particles were dispersed in 2 mL of 1 mM acetic acid solution containing 1% APTS. The mixture was incubated at room temperature with gentle shaking for 30 min. The amino-modified silica nanoparticles were washed with PBS and precipitated by centrifugation at 13,000 rpm for 10 min. The top solvent was discarded. The nanoparticles were redispersed with PBS buffer by sonication. After 3 times washing, two mL DMF containing 0.0231 g glutaric anhydride was used to disperse the functionalized silica nanoparticles and the solution was incubated overnight. This incubation leads to attachment of carboxyl group on the surface of silica nanoparticles²⁵. After washed two times in DMF and one time in water, the nanoparticles were dispersed with a 2 mL aqueous solution containing 0.1 M MES, 10 mM NHS and 10 mM EDC and activated for 1.0 hour. Then the silica nanoparticles were washed in PBS once. The activated nanoparticles were dispersed in 2 mL PBS containing 200 μ L 0.2 mg/mL anti-IL-6 and incubated for 3 hrs. This incubation resulted in the modification of antibodies on the surface of silica nanoparticles. The antibody conjugated nanoparticles were finally washed three times in PBS and dissolved in 1 mL PBS containing 0.1% BSA (PBSB buffer) to have a concentration approximately 2 mg mL⁻¹ and stored in 4 °C until use. The conjugated nanoparticles were diluted 600 times in PBS, and then used for fluorescence characterization with excitation at 450 nm.

2.5. Microarray Fluorescence Immunoassay

Aminosilanated slides were modified with 200 μ L of a 0.3 mg/mL fresh solution of the homobifunctional cross-linker BS³ in PBS (Dulbecco's phosphate buffered saline) for 5 min. The slides were rinsed briefly with 70% ethanol and dried under a stream of N₂ gas. Anti-IL-6 antibody (0.5 mg/mL in PBS) was printed to each spot on the slides with a robotic MicroGrid printer from Apogent Discoveries (Wilmslow, Cheshire, UK). The diameter of each spot was approximately 150 μ m. Each array contains 6 spots (2 rows).

The arrays were then marked with a hydrophobic pen for facilitating to probe the array with small volumes. The hydrophobic barrier marked by the pen held the small-volume samples over the spotted array. During this step, the arrays were allowed to dry for 5 min. Each array was blocked with 30 μ L 1 \times PBS/casein for 1hr. The excess was removed by aspiration. The slides were washed three times (5 min each time) with 0.01 M PBS, 0.05% Tween (PBST) buffer. Each array was covered with 30 μ L of targeted antigen solution with a desired concentration and incubated overnight in a humidified chamber. The excess was removed by aspiration. The slide was again washed three times with PBST buffer. The array was probed with 25 μ L 6-fold diluted antibody conjugated RuDS nanoparticles (2 mg mL⁻¹) for 2 hrs. After removing the excess and washing with PBST buffer three times, the array was further rinsed with deionized water twice and air-dried. Fluorescence image and quantitative detection of the protein microarray was performed with a ScanArray Express HT microarray scanner. An argon laser 488 nm was used for excitation and a filter of 592 nm was programmed for image measurement.

2.6. Specificity of Sandwich Immunoassay

The specificity of sandwich immunoassay was examined with different antigens. Protein microarray protocol was the same as aforementioned except that the target antigen, IL-6, was replaced with six other proteins: IL-1 α , IL-1 β , TNF- α , MMP-2, IgG and 1% BSA. The concentration of the former five proteins used was 500 ng mL⁻¹. The antigens were all diluted in 0.1 \times PBS/casein blocking solution. Fluorescence detection was performed after the completion of the sandwich immunoreactions.

3. Results and Discussion

In this study, RuDS nanoparticles were used as the label for protein microarray analysis of the biomarker IL-6. The formation of the dye encapsulated nanoparticles involves dissolving the dye molecules in the core region, silicate condensation with the dye, and surfactant removal (Fig. 1). The microemulsion solution was prepared by mixing adequate amounts of surfactant, organic solvent and aqueous solution of dye in aqueous ammonia. Aqueous ammonia acts as both a reactant (H_2O) and a catalyst (NH_3) for the hydrolysis of TEOS. As discussed earlier, surfactant CA-520 was used because of the stable microemulsion region that does not require a co-solvent to stabilize the micellar droplets.³⁷ The prepared silica nanoparticles were characterized with TEM and fluorescence spectrometer. Fig. 2 shows the typical TEM image of RuDS nanoparticles. The nanoparticles were uniform in size with a diameter around 50 nm. Careful examination of the TEM image reveals porous features in the particles, most likely due to the presence of the dye molecules trapped inside. The particles have a smaller size likely due to the fast nucleation without the addition of alcohols. Silica particles nucleate in the early reaction period and subsequently grow into final sizes through the continual collection of reacting species. The growth of silica particles followed a size-independent rate such that the shape of particle size distributions was preserved during particle growth,³⁸ but the particle sizes depend on droplet sizes of the micelles as well as the number of nuclei. A fast nucleation rate favors large number of nuclei and therefore smaller particles sizes. The RuDS nanoparticles have a strong emission spectrum at 595 nm with the excitation wavelength at 450 nm. This spectrum matches that of free Rubpy dye (data not show). Serially diluted nanoparticles were subjected to fluorescence intensity analysis. A linear relationship between the concentration of the nanoparticles and the fluorescence intensity was observed (Data not shown). These results indicate that the silica matrix does not have any negative effect on the emission or excitation for the dyes in the nanoparticles. Based on the concentration of silica and dye molecules, we estimated that about 9,000 Rubpy dyes were encapsulated inside silica nanoparticles. The dye concentration used here represents less than 1 wt% relative to the oil (heptane). As compared to Triton X-100, one of the advantages of CA520 surfactant is high solubility of the hydrophilic component in the microemulsion region. Up to 25 wt % of water can be solubilized.³⁰ Therefore we expect a much higher dye concentration can be incorporated in the microemulsion nanoparticles.

Functional groups can be easily attached to silica nanoparticles through silanization for bioapplications. Fig. 3a illustrates the scheme of synthesis of antibody conjugated RuDS nanoparticle. The silica nanoparticles were functionalized with amino groups on the surface by the interaction with APTS. Amino modified silica nanoparticles were subsequently carboxylated with glutaric anhydride in DMF. Carboxylated silica nanoparticles were readily conjugated with anti-IL-6 in the presence of EDC and NHS. This paper utilized a two step synthesis of antibody conjugated nanoparticles-first generating NHS group on the surface of carboxylated silica nanoparticle and then binding the antibody to the activated surface, preventing self conjugation between antibodies if one step was used.

Protein microarray technology shows promise for clinical appreciations because of its high-throughput capability. Here we develop a new approach incorporating one stable RuDS labels with protein microarray technology for the detection of IL-6. Fig. 3b shows the scheme of the sandwich immunoassay on a microarray format with an amino modified glass slide. Primary antibody, anti-IL-6, was printed on the slide with a microarrayer and immobilized on the surface through a cross linker, BS³. Then the antibody modified slides were blocked with $1 \times \text{PBS}/\text{casein}$ to reduce the non-specific binding for the immunoassays. After washing and aspiration, the primary antibody immobilized slide was incubated with antigen, IL-6 to form an antibody/antigen complex. Following the routine washing, the slide was again incubated with secondary anti-IL-6 antibody conjugated RuDS nanoparticle to form sandwich-type immunocomplexes

with the dye-doped nanoparticles as tags. The completed slides were scanned with a fluorescence microarray scanner. The approach was evaluated with artificial IL-6 samples. Each IL-6 solution with a specific concentration covers 1 array (6 spots in 2 rows) in a slide. For easy comparison, only one row of images for each concentration was shown in Fig. 4A and Fig 5. Fig. 4A shows the fluorescence image of protein microarray with different concentrations of IL-6. It can be seen from this figure that the intensity of the fluorescence images increases with increasing antigen concentration from 0.1 ng mL⁻¹ up to 100 ng mL⁻¹. The resulting calibration curve of fluorescence intensity versus IL-6 concentration is linear from 0.1 ng mL⁻¹ to 10 ng mL⁻¹ (Fig. 4B). When the concentration of IL-6 increases to a certain level, the fluorescence intensity starts to level off, indicating that the binding affinity of the immunocomplex reaches saturation. The signals of six replica spots from each concentration are reproducible with a relative standard deviation less than 10%. The control sample without the presence of IL-6 does not have any spots of fluorescence, indicating that there is no nonspecific binding on the surface, which is ascribed to complete blocking of the surface with blocking agents and washing steps.

In order to examine specificity of the immunoassay on the microarray format with the dye-doped nanoparticle labels, six different proteins, IL-1 α , IL-1 β , TNF- α , MMP-2, IgG and BSA were chosen. The solution containing each protein of 500 ng mL⁻¹ was incubated on the anti-IL-6 immobilized slides followed by reaction with anti-IL-6-RuDS conjugates. After the completion of the sandwich immunoreactions, the slides were subject to fluorescence microarray scanner. The fluorescence images of the immunoassay on the slides obtained with different proteins was shown in Fig. 5. It can be seen from Fig. 5 that there were not any fluorescent image spots for the chosen six proteins while clear circles with high intensity of fluorescence appeared for IL-6. It indicates that the approach is very specific and there is no non-specific binding (e.g. cross-reactivity, physical adsorption) on the microarray immunoassay, which is due to the high specific binding capability of the IL-6 antibodies and complete blocking and washing steps.

4. Conclusions

In this paper, we discussed the synthesis of uniform dye doped silica nanoparticles and demonstrate application of the nanoparticle as labels for sensitive detection of IL-6 on a protein microarray format with a fluorescence scanner. The dye encapsulated nanoparticles have bright fluorescence properties and can be easily modified and conjugated with biomolecules. The unique characteristics of RuDS nanoparticles make them applicable in detection of biomarkers. The feasibility of bioassay using RuDS labels in connection with protein microarray technique were studied with IL-6 as a model analyte. RuDS encapsulated silica nanoparticles as labels incorporated with protein microarray technology have high sensitivity for detection of biomarker, e.g. IL-6 and the detection limit can be as low as 0.1 ng mL⁻¹. There was no cross reactivity between co-existing proteins. This approach has good potentials for clinical diagnosis and prognosis of IL-6 related diseases.

Acknowledgments

This work was supported by a laboratory-directed research and development program at Pacific Northwest National Laboratory (PNNL). The work was partly performed at the Environmental Molecular Sciences Laboratory, a national scientific user facility sponsored by the U. S. Department of Energy (DOE) and located at PNNL. PNNL is operated by Battelle for DOE under Contract DE-AC05-76RL01830.

References

1. Sahab ZJ, Semaan SM, Sang Q. Biomarker Insights 2007;2:21.

2. Hernandez-Rodriguez J, Segarra M, Vilardell C, Sanchez M, Garcia-Martinez A, Esteban MJ, Queralt C, Grau JM, Urbano-Marquez A, Palacin A, Colomer D, Cid MC. *Rheumatology* 2004;43:294. [PubMed: 14679293]
3. Timmons BW. *Pediatric Exercise Science* 2006;18:290.
4. Kastelan D, Kastelan M, Massari LP, Korsic M. *Medical Hypotheses* 2006;67:1403. [PubMed: 16844318]
5. Prso IB, Kocjan W, Simic H, Brumini G, Pezelj-Ribaric S, Borcic J, Ferreri S, K. I. M. Mediators of Inflammation, Article ID38210 2007;2007:1.
6. Kimura M, Kavahto Y, Obayashi H, Ohta M, Hara H, Adachi T, Tokunaga D, Hojo T, Hamaguchi M, Omoto A, Ishino H, Wada M, Kohno M, Tsubouchi Y, Yoshikawa T. *J. of Immun* 2007;178:3316. [PubMed: 17312183]
7. Philip M, Rowley DA, Schreiber H. *Seminars in Cancer Biology* 2004;14:433. [PubMed: 15489136]
8. Maggio M, Guralnik JM, Longo DL, Ferrucci L. *The J. of Gerontology* 2006;61A:575.
9. Cesari M, Penninx B, Newman AB, Kritchevsky SB, Nicklas BJ, Sutton-Tyrrell K, Tracy RP, Rubin SM, Harris TB, Pahor M. *Am. J. Cardiol* 2003;92:522. [PubMed: 12943870]
10. May LT, Viguet H, Kenney JS, Ida N, Allison AC, Sehgal PB. *J. Bio. Chem* 1992;267:19698. [PubMed: 1527089]
11. Domingo-Domenech J, Oliva C, Rovira A, Codony-Servat J, Bosch M, Campas C, Dang L, Rolfe M, Ross JS, Gascon P, Albanell J, Mellado B. *Clin. Cancer Res* 2006;12:5578. [PubMed: 17000695]
12. Lee YW, Hirani AA, Kyprianou N, Toborek M. *Inflamm. Res* 2005;54:380. [PubMed: 16273337]
13. Kiecolt-Glaser JK, Preacher KJ, MacCallum RC, Atkinson C, Malarkey WB, Glaser R. *Proc. Natl. Acad. Sci. USA* 2003;100:9090. [PubMed: 12840146]
14. Turner CK, Blieden TM, Smith TJ, Feldon SE, Foster DC, Sime PJ, Phipps RP. *J. Immunol. Meth* 2004;291:63.
15. Drukier AK, Ossetrova N, Schors E, Brown LR, Tomaszewski J, Sainsbury R, Godovac-Zimmermann J. *J. Prot. Res* 2005;4:2375.
16. Liang KZ, Mu WJ. *Anal. Chim. Acta* 2006;580:128. [PubMed: 17723764]
17. Lv L-L, Liu B-C. *Exp. Rev. Prot* 2007;4:505.
18. Urbanowska T, Mangialaio S, Hartmann C, Legay F. *Cell Biol. & Toxicol* 2003;19:189. [PubMed: 12945746]
19. Olle EW, Sreekumar A, Warner RL, McClintock SD, Chinnaiyan AM, Bleavins MR, Anderson TD, Johnson KJ. *Mol. & Cell. Prot* 2005;4:1664.
20. Woodbury RL, Varnum SM, Zangar RC. *J. Prot. Res* 2002;1:233.
21. Santra S, Wang K, Tapeç R, Tan W. *J. Biomed. Opt* 2001;6:160. [PubMed: 11375725]
22. Lian W, Litherland SA, Badrane H, Tan W, Wu D, Baker HV, Gulig PA, Lim DV, Jin S. *Anal. Biochem* 2004;334:135. [PubMed: 15464962]
23. a Liu G, Lin Y. *J. Am. Chem. Soc* 2007;129:10394. [PubMed: 17676734] b Liu G, Wu H, Dohnalkova A, Lin Y. *Anal. Chem* 2007;79:5614. [PubMed: 17600385]
24. Wang J, Liu G, Lin Y. *Small* 2006;2:1134. [PubMed: 17193577]
25. Wang J, Liu G, Engelhard MH, Lin Y. *Anal. Chem* 2006;78:6974. [PubMed: 17007523]
26. Liu G, Wu H, Wang J, Lin Y. *Small* 2006;2:1139. [PubMed: 17193578]
27. Liu G, Wang J, Wu H, Lin Y. *Anal. Chem* 2006;78:7417. [PubMed: 17073407]
28. Han M, Gao X, Su J, Nie S. *Nature Biotech* 2001;19:631.
29. a Wang J. *small* 2005;1:1036. [PubMed: 17193390] b Liu G, Lin Y. *Talanta* 2007;74:308. [PubMed: 18371644]
30. Bruchez JM, Moronne M, Gin p. Weiss S, Alivisatos AP. *Science* 1998;281:2013. [PubMed: 9748157]
31. Smith JE, Medley CD, Tang Z, Shangguan D, Lofton C, Tan W. *Anal. Chem* 2007;79:3075. [PubMed: 17348633]
32. Huo QS, Liu J, Wang LQ, Jiang YB, Lambert TN, Fang E. *J. Am. Chem. Soc* 2006;128:6447. [PubMed: 16683810]
33. Bayrak Y, Iscan M. *Colloid and Surface A : Physicochem. Eng. Aspects* 2005;268:99.

34. Duan D-R, Yang X-J, Huang G-H, Lu L-D, Wang X. *Mat. Lett* 2006;60:1582.
35. Abarkan I, Doussineau T, Smaïhi M. *Polyhedron* 2006;25:1763.
36. Brinker, C.J.; Scherer, G.W. *Sol-Gel Science*. Academic Press; San Diego: 1990.
37. Gratz K, Helmstedt M, Meyer HW, Quitzsch K. *Colloid Polym. Sci* 1998;276:131.
38. Chang CL, Fogler HS. *Langmuir* 1997;13:3295.

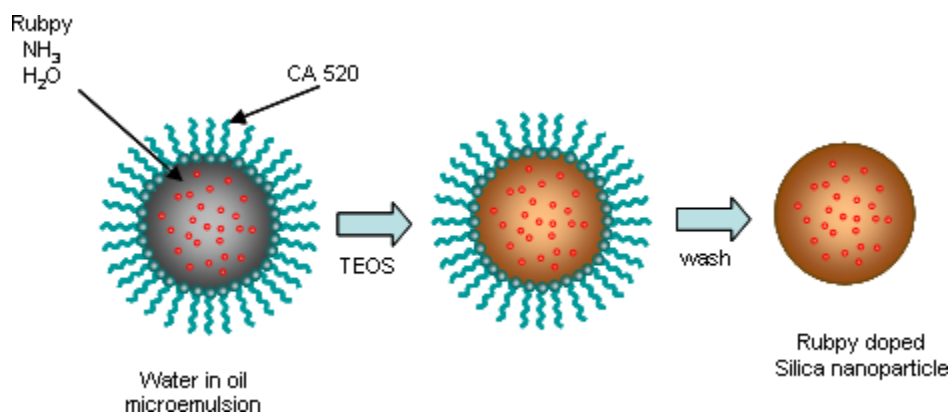


Fig. 1. The schematic illustration of the synthetic procedure for the preparation of Rubpy doped silica (RuDS)

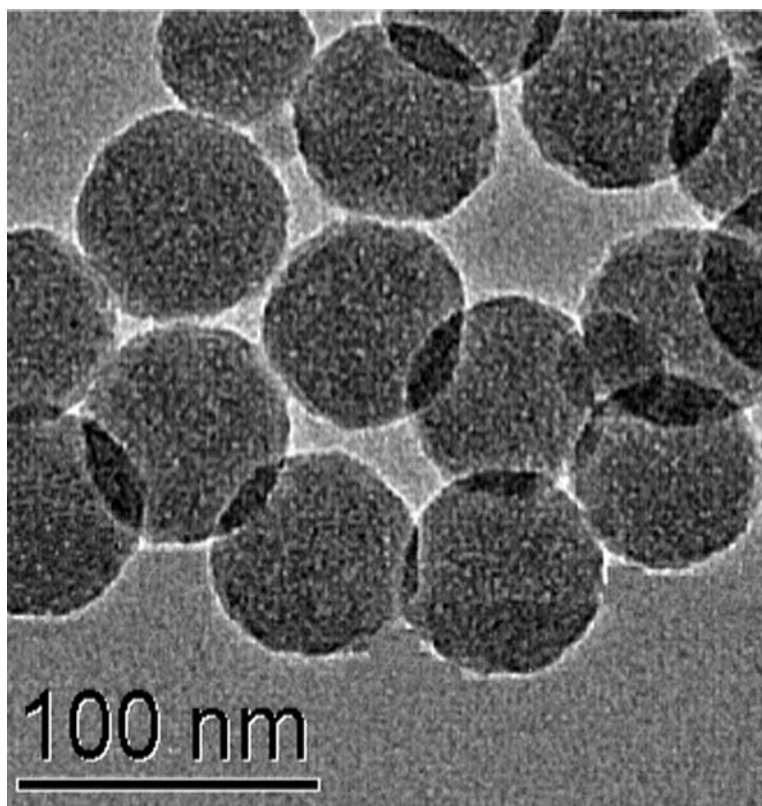


Fig. 2.
Typical TEM image of RuDS nanoparticles.

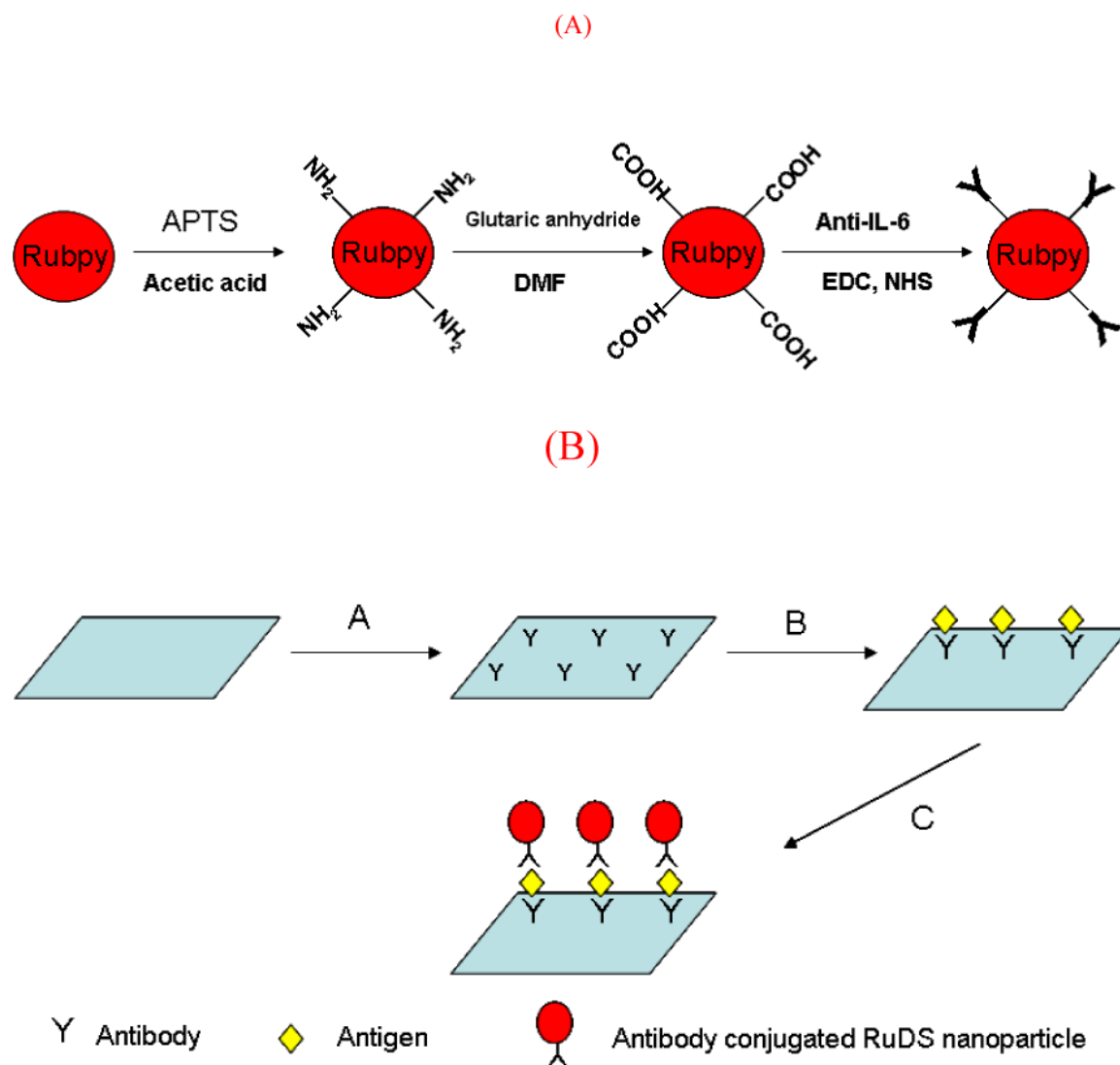
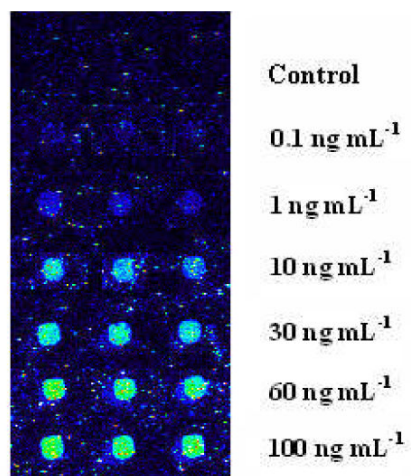
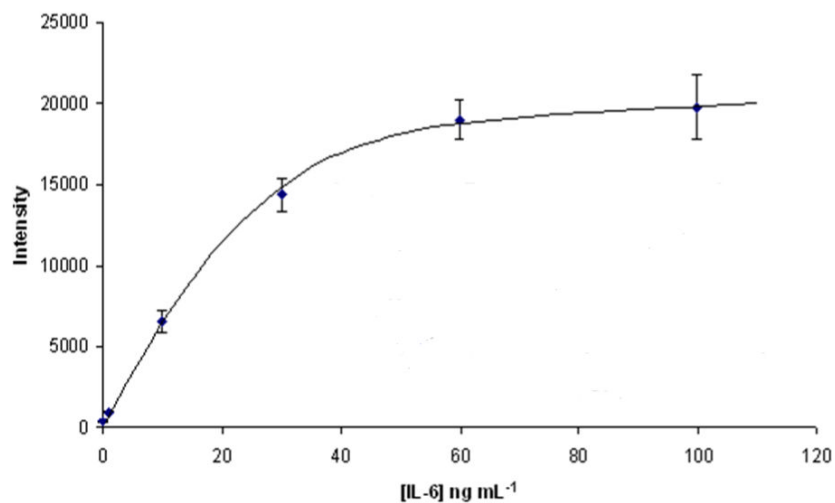


Fig. 3.
 (a) Schematic illustration of the procedure for the preparation of antibody conjugated RuDS nanoparticles. (b) The scheme of the RuDS label-based fluorescent immunoassay of IL-6 on a protein microarray format. A) capture anti-IL-6 antibody was printed on the slide. B) antigen, IL-6, was attached to the slide via antibody/antigen recognition. C) anti-IL-6 antibody-RuDS conjugates was coated on the slide to form a sandwich immunocomplexes with RuDS as tags.



(A)



(B)

Fig. 4. (A) Fluorescence images of protein microarray with different concentrations of antigen, IL-6 (control, 0.1, 1, 10, 30, 60, 100 ng mL⁻¹). (B) Calibration curve of fluorescence intensity versus IL-6 concentration.

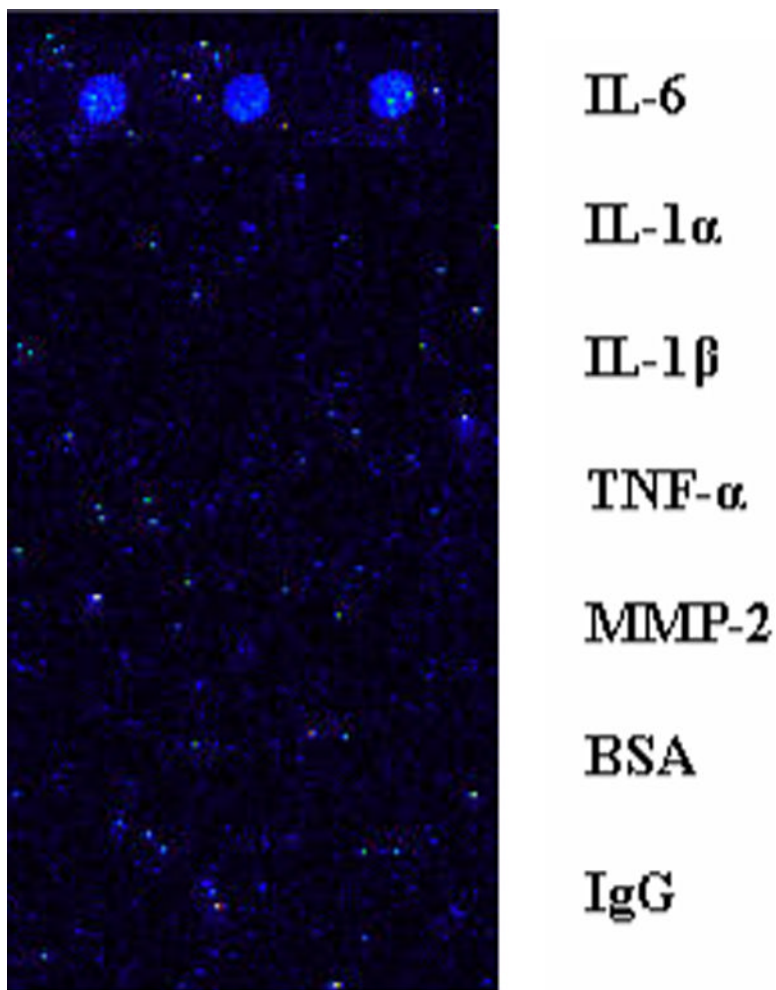


Fig. 5.
The fluorescence images of an IL-6 protein microarray incubated with different antigens, IL-6 (10 ng mL^{-1}) and IL-1 α , IL-1 β , TNF- α , MMP-2, IgG (all in 500 ng mL^{-1}) and 1% BSA.